

Pharmaceutical Nanotechnology

Dry powder aerosol delivery of large hollow nanoparticulate aggregates as prospective carriers of nanoparticulate drugs: Effects of phospholipids

Kunn Hadinoto^{a,*}, Ponpan Phanapavudhikul^a, Zhu Kewu^a, Reginald B.H. Tan^{a,b}

^a A*STAR Institute of Chemical and Engineering Sciences, Singapore 627833, Singapore

^b Department of Chemical & Biomolecular Engineering, National University of Singapore, Singapore 119260, Singapore

Received 5 June 2006; received in revised form 29 August 2006; accepted 6 October 2006

Available online 10 October 2006

Abstract

The present work details the effects of incorporating phospholipids, a major component of lung surfactants, in the formulation of large hollow nanoparticulate aggregates, which are specifically designed to serve as potential carrier particles in inhaled delivery of nanoparticulate drugs. The large hollow aerosol particles ($d_g \approx 10 \mu\text{m}$), whose shells are composed of nanoparticulate aggregates, are manufactured via the spray drying of nanoparticulate suspensions under a predetermined operating condition. Polyacrylate and silica nanoparticles of various sizes (20–170 nm), without loaded drugs, are employed as the model nanoparticles. The effects of increasing the phospholipids concentration in the presence of the nanoparticles, and vice versa, on the degree of hollowness and morphology of the spray-dried particles are investigated. Varying the phospholipids concentration in the presence of a constant amount of nanoparticles is found to influence the degree of hollowness, without significantly affecting the particle size distribution and respirable fine particle fraction, of the aerosol particles. The effects of increasing the phospholipids concentration on the degree of hollowness of the spray-dried particles are found to depend on the size and chemical nature of the nanoparticles.

© 2006 Elsevier B.V. All rights reserved.

Keywords: Dry powder inhaler; Inhaled drug delivery; Pulmonary delivery; Nanoparticulate drugs; Spray drying; Hollow particles

1. Introduction

1.1. Nanoparticulate drugs carriers for dry powder aerosols delivery

Due to rapid advances in nanotechnology, the use of nanoparticulate drugs as therapeutic carriers has become a subject of very active research. Nanoparticulate drugs have an enormous potential in significantly improving the drug systemic bioavailability, which is defined as the rate and extent of therapeutically active drugs that reach the systemic circulation. The high systemic bioavailability of nanoparticulate drugs is attributed to their higher dissolution rate in an aqueous environment, as a result of the larger surface areas compared to their micron-size particles counterpart (Shargel and Yu, 1999; Lee, 2003). Therapeutic agents of nanoparticulate drugs can either be (1) physically dispersed within the matrix of polymer-based carriers

(Govender et al., 1999; Eerikäinen et al., 2003; Raula et al., 2004; Hyvönen et al., 2005; Teixeira et al., 2005), or (2) encapsulated within or loaded on the surface of inert carriers (Cook et al., 2005; Grenha et al., 2005), such that the drug release rate and pattern can be controlled. A wide range of nanoparticulate drugs for oral and parenteral delivery, in the form of nanoparticulate suspensions and nanoparticulate composites, has been investigated, and several of them have already been commercially manufactured (Kipp, 2004).

However, a much less attention has been paid to the dry powder aerosol delivery of nanoparticulate drugs, despite the fact that inhaled dry powder aerosols have been proven to be the effective therapeutic carriers for target-specific treatments of various pulmonary diseases. As the therapeutic agents in an inhaled drug delivery system can evade the first pass hepatic metabolism in the liver, the drug systemic bioavailability is significantly improved (Lalka et al., 1993). As a result, dry powder aerosols have recently become an attractive alternative to oral and parenteral routes for systemic delivery of therapeutic agents, such as insulin, proteins, peptides, which are commonly delivered only through the gastrointestinal tract, or parenterally by

* Corresponding author. Tel.: +65 6796 3858; fax: +65 6316 6183.
E-mail address: kunn.hadinoto-ong@ices.a-star.edu.sg (K. Hadinoto).

either intravenous or intramuscular injections (Pang et al., 2005; Patel et al., 2005).

The current lack of commercial appeal in dry powder aerosol delivery of nanoparticulate drugs is attributed to the fact that (1) nanoparticulate aerosols are predominantly exhaled, and not deposited in the lungs due to their extremely low inertia, and (2) the persisting aggregation problem arising from their small size, which makes their physical handling extremely difficult for the dry powder inhaler (DPI) applications. To circumvent the above problems, novel formulation techniques to manufacture micron-size carrier particles of nanoparticulate drugs have been developed to facilitate delivery of nanoparticulate drugs by inhalation (Tsapis et al., 2002; Sham et al., 2004; Grenha et al., 2005; Hadinoto et al., 2006). In particular, large hollow carrier particles, whose shells are composed of nanoparticulate aggregates that can potentially be loaded with therapeutic agents, have been manufactured by Tsapis et al. (2002) and Hadinoto et al. (2006), by employing the spray drying technique. The nanoparticulate aggregates are designed to disassociate into primary nanoparticles in the aqueous environment of the lungs, where the therapeutic agents entrapped in the nanoparticles are released and subsequently delivered to a specific pulmonary target or to the systemic circulation.

The large hollow nanoparticulate aggregates exhibit a large geometric diameter ($d_g \approx 10 \mu\text{m}$), and a small aerodynamic diameter ($1 \mu\text{m} \leq d_a \leq 5 \mu\text{m}$) attributed to the low particle density. The aerodynamic diameter (d_a) is defined as the diameter of a unit density spherical particle that settles through the air with a velocity equal to that of the particle in question (Eq. (1)), and is widely used to characterize the distance traveled by the inhaled particles in human respiratory airways.

$$d_a = d_g \sqrt{\frac{\rho_c}{\rho_s}} \quad (1)$$

where $\rho_s = 1 \text{ g/cm}^3$, d_a and d_g the particle aerodynamic and geometric diameters, respectively, and ρ_c is the effective particle density defined as the mass of a particle divided by its total volume including the open and close pores. Owing to their physical characteristics, the large hollow nanoparticulate aggregates possess two valuable attributes for use in a dry powder inhaler, i.e. (1) the large geometric size reduces their tendency to aggregate, which consequently improves the flowability of the carrier particles off the inhaler (French et al., 1996), and (2) by virtue of their small aerodynamic diameters ($d_a \leq 5 \mu\text{m}$), the deposition of the carrier particles in the mouth and throat regions is minimized, so that they are capable of reaching the targeted alveolar region of the lungs more effectively (Tsapis et al., 2002).

Moreover, in the dry powder aerosol delivery, the inhaled particles are subjected to the phagocytic clearance mechanism in the alveolar region of the lungs by the scavenging alveolar macrophages. The lung phagocytosis is most significant for particles having $1 \mu\text{m} \leq d_g \leq 2 \mu\text{m}$, and diminishes for particles having smaller or larger sizes (Ahsan et al., 2002; Makino et al., 2003). As a result, particles having large geometric diame-

ters ($d_g \geq 5 \mu\text{m}$) have been found to exhibit a higher systemic bioavailability than their smaller size counterparts (Edwards et al., 1997), which signifies another valuable attribute of the large hollow nanoparticulate aggregates.

1.2. The roles of phospholipids in the large hollow particles formulation

Inclusion of phospholipids, which constitutes 80–90% of the major components in lung surfactants, at the surface of the inhaled particles has been found to lead to a significant decrease in the phagocytic uptake of the inhaled particles. In the presence of the phospholipids at the surface of the inhaled particles, the adsorption of opsonic proteins, which are responsible for phagocytosis, is reduced (Evora et al., 1998; Jones et al., 2002). In addition, the presence of the phospholipids at the particle surface has been found to lead to an improvement in the respirable fine particle fraction ($d_a \leq 5 \mu\text{m}$) of the inhaled particles, which is attributed to the reduced surface hygroscopicity of the phospholipids-enriched surfaces (Sacchetti and Van Oort, 1996; Bosquillon et al., 2001). The many benefits that arise from the presence of the phospholipids at the surface of the inhaled particles hence are well recognized. In the present work, an experimental study is conducted to investigate the effects of the phospholipids inclusion in the large hollow nanoparticulate aggregates formulation.

In the drying of a nanoparticulate suspension, evaporation of the liquid from the surface of the atomized droplets during the spray drying process leads to the supersaturated particles at the receding liquid–vapor interface being exposed. Because the surface energy of the solid–vapor interface is greater than the liquid–vapor interface, the exposed particles tend to move inward and the liquid tends to spread from the interior of the droplet to prevent such an increase in the energy (Scherer, 1990; Liang et al., 2001). The large hollow nanoparticulate aggregates are obtained by spray drying of nanoparticulate suspensions at a fast convective drying rate, where the time for the liquid to evaporate is much less than the time required for the supersaturated nanoparticles at the interface to migrate back toward the droplet center. A fast drying rate is ensured when the local Peclet number Pe (Eq. (2)), which signifies the relative importance of the time scale for diffusion (R^2/D_s) and convective drying (τ_D), is much greater than unity.

$$Pe = \frac{R^2}{\tau_D D_s} \quad (2)$$

where R , τ_D , and D_s are the droplet radius, drying time, and diffusion coefficient, respectively. When $Pe \gg 1$, the migration of the nanoparticles at the interface toward the droplet center is insufficient to keep up with the convective drying rate resulting in the shell formation. Once the shell formation begins, the driving force for the formation of nanoparticulate aggregates in the shell of the hollow particles is the shrinking surface area of the droplet as the liquid evaporates, forcing the nanoparticles to come close to each other. The capillary force that is generated by a meniscus

formed in the gap between the nanoparticles pulls the liquid outward, and accordingly pushes the nanoparticles even closer, resulting in the formation of nanoparticulate aggregates after drying.

In the presence of the phospholipids, however, the nanoparticles ought to compete with the phospholipids to occupy the liquid–vapor interface in which prior to drying is preferentially occupied by the phospholipids due to their surfactant nature. Therefore, a smaller area is available for the nanoparticles to aggregate as a result of the competitive adsorption at the interface, which would consequently influence the shell formation process. It is analogous to the competitive adsorption between the protein and surfactant molecules observed in the works of Maa et al. (1998) and Adler et al. (2000), where the competitive adsorption led to a transformation in the surface morphology of the spray-dried proteins particles. The surface chemistry of the spray-dried particles became dominated by the surfactant that acted as the stabilizing force at the liquid–vapor interface of the atomized droplets, resulting in an exclusion of the protein molecules from the particle surface. In addition, Tsapis et al. (2002) have reported that spray drying of a phospholipids solution at a fast drying rate leads to a spontaneous formation of large hollow porous particles, whose shells are composed of colloidal aggregates of the phospholipids. The result indicates that the phospholipids behave in a similar manner as the nanoparticles upon drying.

The competitive adsorption at the interface between the phospholipids and the nanoparticles, as well as the possible formation of the colloidal aggregates of the phospholipids, is hypothesized to influence the shell formation of the large hollow nanoparticulate aggregates. To evaluate the hypothesis, a study on the effects of varying the phospholipids concentration on the morphology and degree of hollowness of the large hollow nanoparticulate aggregates is conducted. In addition, the effects of varying nanoparticles concentration, which have been reported in Hadinoto et al. (2006), are re-examined in the presence of the phospholipids. To examine the influence of the chemical nature and size of the nanoparticles on the results, silica and biocompatible polyacrylate nanoparticles having a wide range of sizes (20–170 nm) are used in the experiments. The results of our study provide a comprehensive insight into the spray drying formulation of the large hollow nanoparticulate aggregates intended for the dry powder aerosol delivery of nanoparticulate drugs.

2. Materials and methods

2.1. Materials

The monomers for the synthesis of the polyacrylate nanoparticles, i.e. methyl methacrylate (MMA, purity $\geq 99\%$), butyl acrylate (Ba, purity $\geq 99\%$), acrylic acid (AA, purity $\geq 99\%$), methoxy(polyethylene glycol)methacrylate (MeOPEGMA, MW = 2000), and the initiator 4,4-azobis(4-cyanovaleric acid) (carboxy ADIB, purity $\geq 75\%$) are purchased from Sigma–Aldrich, except for the MeOPEGMA, which is kindly supplied by Cognis Performance Chemicals (UK). Aqueous suspensions of colloidal silica Ludox TM-40 (pH 9.0; 40%, w/v; 20 ± 10 nm), ethyl acetate (purity $\geq 99.5\%$), and Trizma base (purity $\geq 99.9\%$) are purchased from Sigma–Aldrich. Phospholipids S100 (95% phosphatidylcholine from fat free soybean lecithin) is purchased from Lipoid GmbH (Ger-

many). Ultra-pure water and ethanol analytical grade are used in the experiments.

2.2. Methods

2.2.1. Preparation of polyacrylate nanoparticles

Polyacrylate is prepared by a solution tetrapolymerization of MeOPEGMA, MMA, Ba, and AA in the proportions 15/69/11/5 (% w/w) as described in Phanapavudhikul et al. (2002). Ethyl acetate and ethanol are used as the solvents. The polymer is converted into polyacrylate nanoparticles by a solvent replacement technique. The nanoparticles exhibit steric colloidal stability arising from the MeOPEGMA component. Briefly, dissolve 0.15 g carboxy ADIB in 15 mL ethanol and add 55 mL ethyl acetate. Reflux the solution for 45 min at 90°C in a water-cooled reflux condenser. Separately, prepare the feed solution by dissolving 0.13 g carboxy ADIB in 6 mL ethanol and add 12.7 g MeOPEGMA. Next, mix MMA, Ba, and AA monomers according to their weight fraction in a separate beaker. Make up the volume of both feed solutions to 50 mL by adding ethanol. Add the two feed solution drop-wise into the solution that has been refluxed for 45 min, and let the polymerization run for about 2 h at 90°C . At the end of the polymerization, the temperature is maintained at 90°C to partially evaporate the ethyl acetate, while 50–00 mL ethanol is continuously added to prevent the polymers from drying out. Next, the solvent is displaced by adding water drop-wise at 70°C inducing a macromolecular rearrangement of the polymers to form colloidally-stable particles, which is evident as the solution gradually becomes cloudy in its appearance. Continue heating at 70°C to let the remaining ethanol evaporate. Lastly, the nanoparticulate suspension in water is dialyzed for 1 week to remove excess monomers and solvents. A wide range of nanoparticles sizes can be obtained by varying the amount of ethanol added after the polymerization steps.

2.2.2. Preparation of nanoparticulate suspensions with phospholipids

In the presence of the phospholipids, nanoparticulate suspensions of silica (40%, w/v) and polyacrylate (4%, w/v) are prepared by (1) dissolving the desired amount of phospholipids in 20 mL of ethanol and (2) mix the resulting solution with silica or polyacrylate nanoparticles that have been dispersed in 180 mL ultra-pure water. In the case of silica nanoparticles, Trizma base is added into the water to ensure colloidal silica stability prior to the addition of the silica nanoparticles. The resulting 200 mL nanoparticulate suspension is spray dried immediately after its preparation.

2.2.3. Spray drying of nanoparticulate suspensions

B-290 Mini Spray Dryer (Büchi, Switzerland) equipped with an inert loop B-295 is employed in the experiments. The B-290 spray dryer operates on the principle of a two-fluid atomizer. In a two-fluid atomizer, compressed gas, either air or nitrogen used only when ethanol is involved, flow parallel in a co-axial nozzle to atomize the sprayed liquid at an elevated temperature in the drying chamber. The spray-dried particles exiting the drying chamber are passed to a cyclone separator, where the gas is exhausted after filtering and the dried particles are collected. The nozzle orifice diameter used in the experiment is 1.5 mm. The adjustable parameters in the experiments are the inlet temperature, the compressed gas flow rate, the aspirator suction rate and the feed flow rate. A wide range of experimental conditions have been investigated in Hadinoto et al. (2006) in order to find an optimal spray drying operating condition that leads to the formation of large hollow particles. The following spray drying operating condition is employed in the present work for both the polyacrylate and silica nanoparticles: inlet temperature of 105°C , compressed air or nitrogen flow rate of 250 L/h, and feed rate of 4.0 mL/min. The resulting outlet temperature at the above operating condition is approximately 60°C .

2.2.4. Particle characterizations: size, density, morphology, surface chemistry

In the sample preparation of the spray-dried particles for characterizations, the particles are stored in a desiccator for a 48-h period prior to the analysis. The size of the nanoparticles is measured by dynamic light scattering, also known as photon correlation spectroscopy, using Zetasizer Nano-ZS (Malvern, UK). The geometric and aerodynamic diameters of the spray-dried particles are determined

by light diffraction using Particle Size Analyzer MS2000 (Malvern) and time-of-flight measurement using Particle Size Distribution Analyzer PSDA 3603 (TSI, USA), respectively. The respirable fine particle fraction is determined using a two-stage Anderson Cascade Impactor (Thermo Andersen, USA) equipped with a pre-separator designed to separate particles with aerodynamic diameters larger than 10 μm . The fractions of particles with aerodynamic diameters below 9.0 μm and below 4.7 μm at an inhalation flow rate of 28.3 L/min are determined from the weight of particles deposited on each stage, which has been calibrated to yield accurate measurements of d_a at 28.3 L/min.

The true and tap densities of the spray-dried particles are determined by Ultracpynometer 1000 (Quantachrome, USA) and Autotap density meter (Quantachrome), respectively. The effective particle density ρ_e is subsequently determined from the tap density, which is approximately a 21% underestimate of the effective particle density for a perfect packing (Vanbever et al., 1999). The degree of hollowness (ψ) of the spray-dried particles is defined as the ratio of the effective density ρ_e to the true density ρ_{true} . The morphologies of the spray-dried particles and polyacrylate nanoparticles are examined using a Scanning Electron Microscope (SEM) model JSM-6700F (JEOL, USA). Transmission Electron Microscope (TEM) model Tecnai-TF-20 (FEI Company, USA) is used to examine the shell thickness of the large hollow nanoparticulate aggregates. For TEM imaging of the spray-dried particles, the sample is prepared by wetting the copper grid prior to sprinkling the particles, and is allowed to dry in a desiccator prior to the analysis.

To verify for the presence of the phospholipids on the surface of the spray-dried particles, a surface chemistry analysis by means of X-Ray Photoelectron Spectrometer (XPS) model ESCALAB 250 (Thermo Electron, USA) is conducted. The XPS can detect the presence of chemical elements located less than 5 nm below the particle surface. A survey spectrum is recorded over a binding energy range of 0–1100 eV to detect surface existence of the phosphor element, which only exists in the phospholipids. Lastly, a Powder X-Ray Diffraction (PXRD, Bruker, UK) analysis is conducted to examine whether the inclusion of the phospholipids leads to a physical-state transformation of the amorphous spray-dried particles, which would consequently influence the stability and solubility of the spray-dried particles.

2.2.5. Test of statistical significance

The statistical significance of the relationships among the data from different experimental groups is evaluated using the *t*-test statistical method. In particular, the statistical test is conducted to evaluate whether the reported effects of varying the nanoparticles and phospholipids concentrations on the morphology and degree of hollowness of the particles are statistically significant (instead of due to a random occurrence). The details of the *t*-test analysis are provided in the Appendix A.

3. Results and discussion

3.1. Formation of large hollow nanoparticulate aggregates with phospholipids

3.1.1. Surface chemical composition

The XPS analysis is conducted for the spray-dried particles of the 160 ± 40 nm polyacrylate nanoparticles at 33% phospholipids concentration. The phospholipids concentration is determined from the ratio of the phospholipids mass to the total solid mass, which includes both the masses of the nanoparticles and the phospholipids. The XPS survey spectra (0–1100 eV) record the presence of only oxygen (O 1s 533 eV) and carbon (C 1s 285 eV) at the surface of the spray-dried particles. Relative to carbon and oxygen, phosphor makes up only a small fraction of the phosphatidylcholine molecules, which explains the absence of the phosphor peak in the survey spectra. A closer look in the binding energy range of 120–140 eV, however, reveals the existence of the phosphor element (P 2p 130 eV) at the surface.

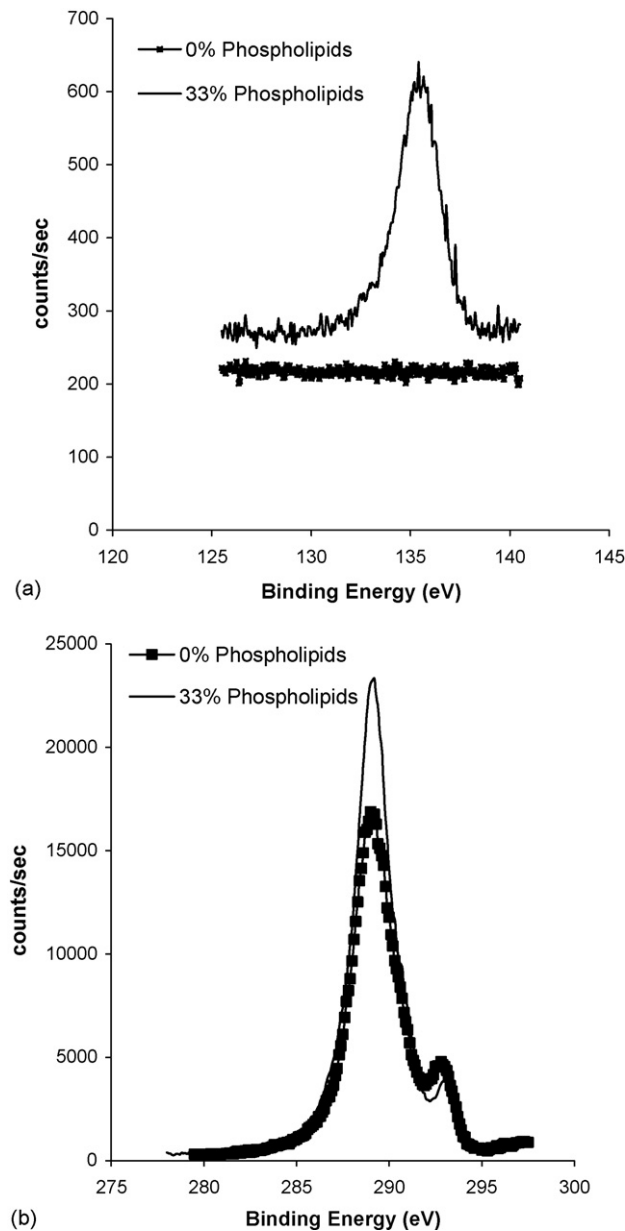


Fig. 1. The XPS spectra of the spray-dried particles for the 160 ± 40 nm polyacrylate nanoparticles at 33% phospholipids concentration: (a) P 2p 130 eV and (b) C 1s 289 eV.

Fig. 1a displays a small peak around 135 eV in the spectra of the spray-dried particles at 33% phospholipids concentration, which is absent in the spectra of the spray-dried particles without the phospholipids.

Because the phosphor peak is very weak, the presence of the phospholipids at the surface of the spray-dried particles is reaffirmed using the C 1s spectra of the same particles. The C 1s spectra (Fig. 1b) indicate that the inclusion of the phospholipids leads to a higher intensity over the binding energy range of 288–290 eV, resulting from the presence of additional carbons of the phospholipids at the surface. For a wide range of phospholipids concentrations, the PXRD results indicate that the spray-dried particles remain completely amorphous in the presence of the phospholipids. Therefore, the inclusion of the

phospholipids influences only the surface composition, but not the physical state, of the large hollow nanoparticulate aggregates.

3.1.2. Morphology and degree of hollowness

In the present work, nanoparticulate suspensions of the polyacrylate and silica nanoparticles having a wide range of sizes (i.e. polyacrylate: 50 ± 30 , 70 ± 40 , 160 ± 40 , and 170 ± 80 nm, and silica: 20 ± 10 nm) are spray dried in the presence of the phospholipids. At the current spray drying operating conditions, the Pe number is approximately equal to 1000, which signifies a fast drying rate necessary to form the large hollow nanoparticulate aggregates. An SEM image of the spray-dried particles of the 50 ± 30 nm polyacrylate nanoparticulate suspension at a solid concentration of 1.1% (w/w), with 27% phospholipids concentration, is provided in Fig. 2a. The reported values of the solid concentration are determined from the ratio of the solid mass (i.e. nanoparticles and phospholipids) to the total mass of the suspension. A mixture of large hollow dimpled spherical particles about 10–15 μm in diameter and fine spherical particles less than 5 μm in diameter is produced. The mean d_g (by volume) of the spray-dried particles is 11 ± 3 μm (median = 8; mode = 10 μm), and the mean d_a (by volume) is 2.9 ± 1 μm . The experimental uncertainties of the measured d_g and d_a , based on three independent measurements, are approximately 10% and 5%, respectively. By comparison with the results of Hadinoto et al. (2006), the SEM image indicates that the inclusion of the phospholipids in the formulation does not noticeably influence the resulting morphology, or the particle size distribution, of the large hollow nanoparticulate aggregates.

The hollowness of the spray-dried particles is evident in the lower value of their d_a compared to the d_g , and also in their low effective particle density ($\rho_e = 0.26$ g/cm³) relative to the true density ($\rho_{\text{true}} = 1.3$ g/cm³). Fig. 2b shows a TEM image of the spray-dried particles, whose shell (thickness ≈ 1 μm) exhibits darker areas than the interior, as fewer electrons are transmitted through, reaffirming the hollowness of the particles. The degree of hollowness of the spray-dried particles is defined as the ratio of the effective density to the true density of the particles ($\rho_e/\rho_{\text{true}}$), which is proportional to $(d_a/d_g)^2$ (as indicated by Eq. (1)). Therefore, the degree of hollowness can be quantified by either measurements of (1) the tap and true densities (ψ^{tap}), or (2) the aerodynamic and geometric diameters (ψ^{dia}). Previous works on the dry powder formulation of hollow porous particles for inhaled drug delivery (i.e. Vanbever et al., 1999; Dellamary et al., 2000; Bosquillon et al., 2001; Steckel and Brandes, 2004; Hadinoto et al., 2006) have exclusively relied on the former in determining the degree of hollowness of the particles. In the present work, the degree of hollowness is reported using both measurements. The experimental uncertainties for the degree of hollowness, determined from the tap density (ψ^{tap}), are approximately 13% and 10% for the polyacrylate and silica nanoparticles, respectively.

Particles with a similar morphology are obtained from the spray drying of the 70 ± 40 nm polyacrylate nanoparticulate suspension at a solid concentration of 3.0% (w/w), with 21% phospholipids concentration. Fig. 3a and b shows SEM images

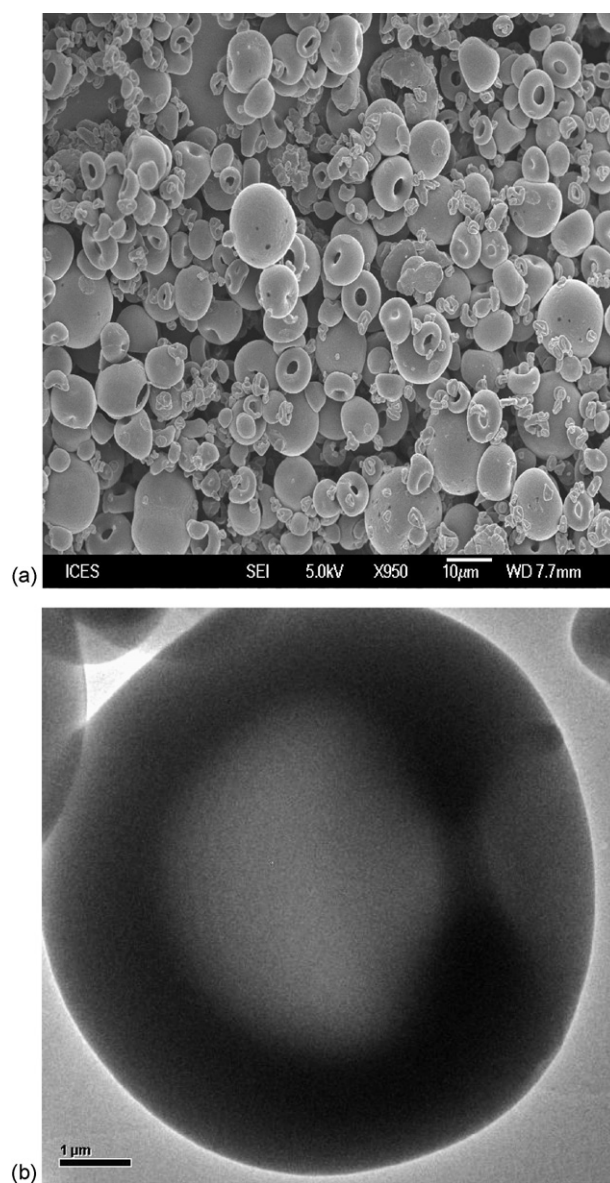


Fig. 2. Spray-dried particles of the 50 ± 30 nm polyacrylate nanoparticles at a solid concentration of 1.1% (w/w) and 27% phospholipids: (a) SEM image of the large hollow nanoparticulate aggregates and (b) TEM image of the shell thickness.

of the spray-dried particles, where a close-up view of the surface (Fig. 3b) clearly shows that the shell of the hollow particle is composed of the aggregates of the polyacrylate nanoparticles. The mean d_g and d_a of the spray-dried particles are 7 ± 2 μm (median = 6; mode = 6 μm) and 2.7 ± 1 μm , respectively, and the effective particle density is approximately 0.19 g/cm³. For all the spray-dried particles, the nanoparticulate aggregates easily disassociate into the primary nanoparticles in an aqueous environment. As previously reported in Hadinoto et al. (2006), the Zetasizer measurement of the redispersed polyacrylate nanoparticles indicates that the nanoparticles preserve their primary particle size after spray drying, which is attributed to the outlet drying temperature of the spray dryer being lower than the glass transition temperature of the polymer ($T_g = 65$ °C).

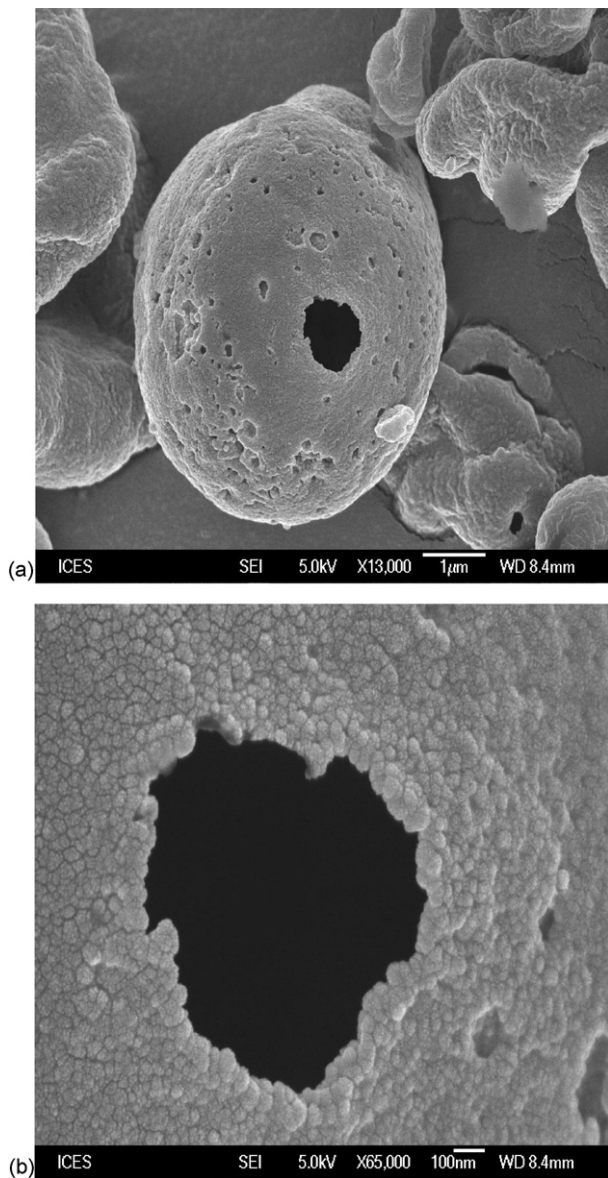


Fig. 3. Spray-dried particles of the 70 ± 40 nm polyacrylate nanoparticles at a solid concentration of 3.0% (w/w) and 21% phospholipids: (a) SEM image of the large hollow nanoparticulate aggregates and (b) SEM image of the nanoparticulate aggregates at the surface.

3.2. Effects of nanoparticles concentration in the presence of phospholipids

In the absence of the phospholipids, Hadinoto et al. (2006) reported that the effects of increasing the nanoparticles concentration on the degree of hollowness of the large hollow nanoparticulate aggregates varied only for nanoparticles of different chemical nature, but not for different size nanoparticles of the same chemical nature. For the spray-dried polyacrylate particles, the degree of hollowness, determined from the tap density measurement (ψ^{tap}), was found not to be affected by the change in the nanoparticles concentration, provided that the nanoparticles concentration was above the concentration threshold necessary for the large hollow nanoparticulate aggregates formation. On the other hand, the degree of hollowness (ψ^{tap})

of the spray-dried silica particles was shown to decrease with increasing nanoparticles concentration. In addition, for nanoparticles of the same chemical nature, the magnitude of the degree of hollowness and diameters (both d_g and d_a) was found to be independent of the size of the nanoparticles.

In the presence of the phospholipids, however, the aforementioned competitive adsorption between the phospholipids and the nanoparticles are expected to influence the outcome of varying the nanoparticles concentration. In the present work, nanoparticulate suspensions of the 70 ± 40 and 170 ± 80 nm polyacrylate nanoparticles are spray dried in the presence of a constant amount of the phospholipids (1 g/200 mL). Two different sizes of nanoparticles are used in the experiments to examine the effects of the size of the nanoparticles on the outcome of the study. A summary of the experimental results for the degree of hollowness and the particle size distribution is provided in Table 1.

For both the 70 ± 40 and 170 ± 80 nm nanoparticles, Fig. 4a indicates that the variations in the degree of hollowness (ψ^{tap}) of the spray-dried particles, as a function of the nanoparticles concentration, are still within its experimental uncertainties. The geometric diameter of the spray-dried particles is shown in Fig. 4b to decrease with increasing nanoparticles concentration, whereas the aerodynamic diameter is not affected by the change in the nanoparticles concentration. However, when the degree of hollowness of the spray-dried particles is calculated from the values of $(d_a/d_g)^2$, Fig. 4c shows that the degree of hollowness (ψ^{dia}) initially decreases with increasing nanoparticles concentration, before it starts to increase at higher nanoparticles concentrations ($\geq 2.4\%$, w/w). The discrepancy between the trend in the degree of hollowness determined from the tap density (ψ^{tap}) and that from the diameter measurement (ψ^{dia}) can be explained by examining the trend in the particle size distribution of the spray-dried particles as a function of the nanoparticles concentration.

A closer look at the particle size distribution results (Table 1) reveals that increasing the nanoparticles concentration leads to an increase in the amount of fine particles ($d_g \leq 5 \mu\text{m}$) being produced. The mean d_g of the spray-dried particles decreases from approximately 12–14 to 7–8 μm for the 70 ± 40 nm nanoparticles, and from approximately 10 to 4 μm for the 170 ± 80 nm nanoparticles. The shift in the median and mode values of the particle size distribution to lower diameter values (Table 1) reaffirms the increased production of fine particles at high nanoparticles concentrations. The increased fine particles production is attributed to the decrease in the average size of the atomized droplets at high solute concentrations, resulting from the change in the physical properties of the liquid feed, i.e. surface tension, density (Hinds, 1982; Moon et al., 2000). The tap density measurement is best used to estimate the bulk or effective density of the particles when the tapping of the particles is not affected by the interparticle forces acting on the particle surface (i.e. non-cohesive). The increased presence of the fine particles results in the packing density being significantly affected by the particle cohesiveness, as the inertial force exerted by tapping is not adequate to overcome the interparticle force. Accordingly, when a significant amount of fine particles is present, the tap density

Table 1
A summary of the experimental results for the effects of the nanoparticles concentration in the presence of the phospholipids

Nanoparticles	Solid concentration (% _v , w/w)	Nanoparticles concentration (% _v , w/w)	Phospholipids (% of total solid)	ρ_e/ρ_{true}^a ($\pm 13\%$)	ρ_e/ρ_{true}^b ($\pm 10\%$)	Mean d_g (μm) ($\pm 10\%$)	Median d_g (μm)	Mode d_g (μm)	d_a (μm) ($\pm 5\%$)
Polyacrylate 70 \pm 40 nm	1.3	0.5	63	0.12	0.04	14.4	10.5	7.1	3.4
	1.7	1.0	42	0.12	0.03	11.8	7.0	5.7	2.2
	2.2	1.5	31	0.13	0.15	6.7	5.0	4.6	3.0
	3.0	2.4	21	0.15	0.11	7.3	5.7	5.7	2.7
	3.8	3.2	16	0.14	0.10	8.4	6.0	5.7	2.9
Polyacrylate 170 \pm 80 nm	1.3	0.5	63	0.14	0.09	9.5	9.0	8.7	3.2
	1.7	1.0	42	0.14	0.32	4.2	3.0	3.7	2.7
	2.2	1.5	31	0.16	0.40	4.0	2.0	3.0	2.9
	3.0	2.4	21	0.24	0.17	5.7	4.5	4.6	2.7

^a From tap density measurement, ψ^{tap} .

^b From the ratio of $(d_a/d_g)^2$, ψ^{dia} .

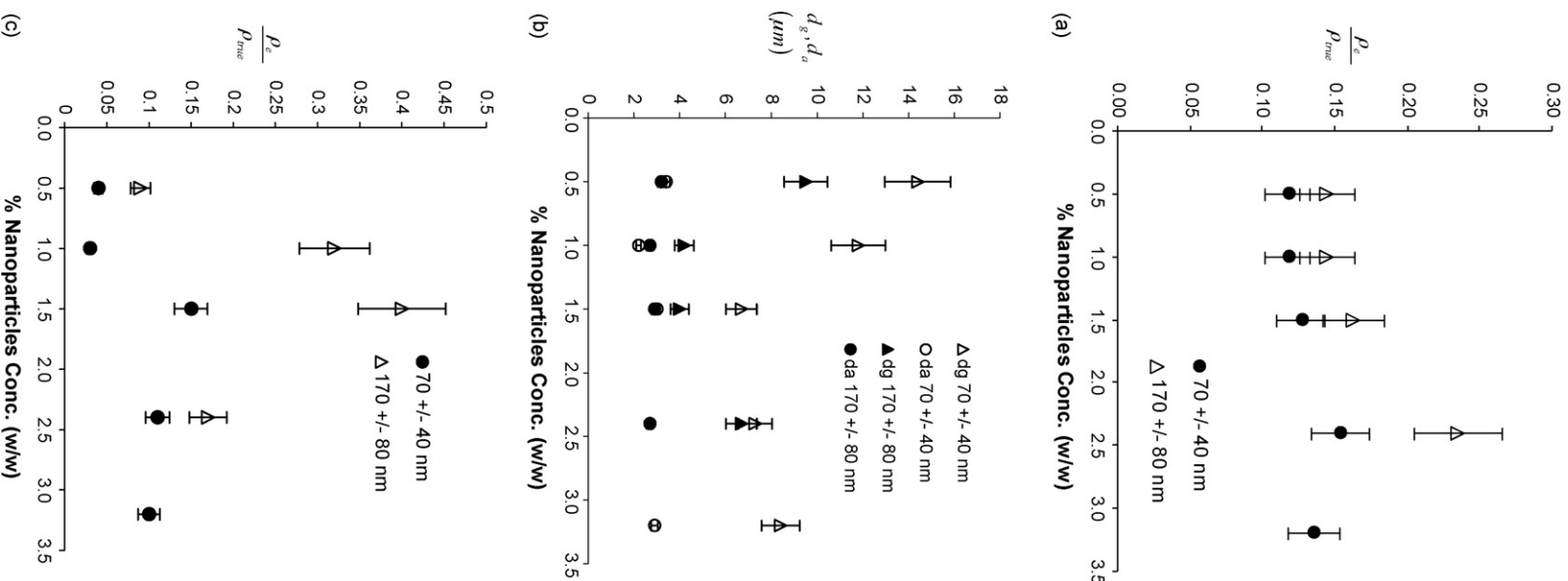


Fig. 4. Spray-dried particles of the 70 \pm 40 and 170 \pm 80 nm polyacrylate nanoparticles: (a) the degree of hollowness determined from the tap density, ψ^{tap} , (b) geometric and aerodynamic diameters and (c) the degree of hollowness determined from the diameters, ψ^{dia} .

measurement is unable to accurately capture the variation in the degree of hollowness of the spray-dried particles.

In a further evaluation, the degree of hollowness of the spray-dried particles reported in Hadinoto et al. (2006), which was determined from the tap density measurement and without the phospholipids, is recalculated using the reported values of $(d_a/d_g)^2$. For both the silica and polyacrylate nanoparticles, the results (Table 2) indicate that the degree of hollowness (ψ^{dia}) decreases with increasing nanoparticles concentration, which is again in contrast to the results obtained from ψ^{tap} . Furthermore, contrary to the polyacrylate nanoparticles, the tap density measurement of the spray-dried silica particles was able to capture the decrease in the degree of hollowness. The reason was because the increased production of fine particles at high nanoparticles concentrations was not observed in the spray drying of the silica nanoparticles (Hadinoto et al., 2006).

To explain for the initial decrease in the degree of hollowness (ψ^{dia}) with increasing nanoparticles concentration ($\leq 2.4\%$, w/w), a TEM image of the fine particles ($d_g \approx 4 \mu\text{m}$), produced from the spray drying of the $170 \pm 80 \text{ nm}$ nanoparticles at a solid concentration of 1.7% (w/w), is shown in Fig. 5. The TEM image indicates that the ratio of the shell thickness to the particle radius of the fine particles is higher than that of the large hollow particles (Fig. 2b). The increased shell thickness of the fine particles is attributed to the decrease in the size of the atomized droplets at high nanoparticles concentrations, such that the nanoparticles travel a shorter radial distance to migrate toward the droplet center. As a result, a more uniform nanoparticles concentration exists within the drying droplet, leading to the formation of almost-solid fine spray-dried particles.

At nanoparticles concentrations $\geq 2.4\%$ (w/w), however, Fig. 4c indicates a subsequent increase in the degree of hollowness (ψ^{dia}) for both the 70 ± 40 and $170 \pm 80 \text{ nm}$ nanoparticles. A similar trend is observed with the $140 \pm 10 \text{ nm}$ polyacrylate nanoparticles ($\geq 3.2\%$, w/w) and the $20 \pm 10 \text{ nm}$ silica nanoparticles ($\geq 1.88\%$, w/w) (Table 2). The increase in the degree of hollowness of the spray-dried particles is accompanied by a slight increase in the average geometric diameter of the spray-

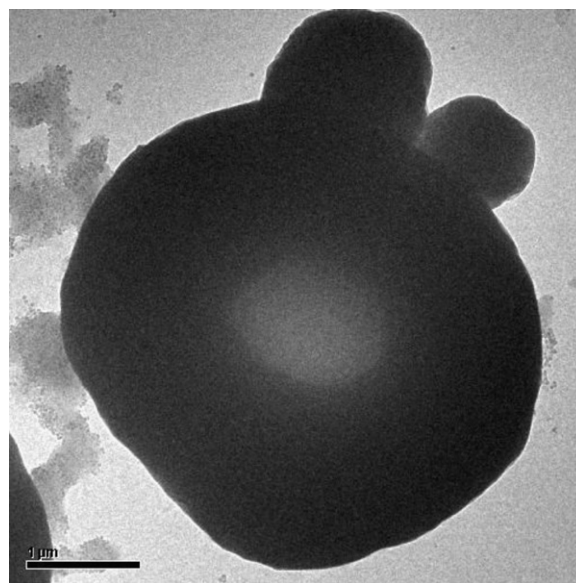


Fig. 5. A TEM image of the spray-dried fine particles for the $170 \pm 80 \text{ nm}$ polyacrylate nanoparticles at a solid concentration of 1.7% (w/w) and 42% phospholipids.

dried particles, signifying a diminished production of the fine particles. In the spray drying using a two-fluid atomizer, the size of the atomized droplet is proportional to the viscosity of the suspension (Lukasiewicz, 1989). Therefore, the increase in the average particle size is postulated due to an increase in the viscosity of the nanoparticulate suspension at nanoparticles concentrations above 2.4% (w/w).

In the presence of the phospholipids, our results indicate that the trend in the degree of hollowness (ψ^{dia}) as a function of the nanoparticles concentration is in accordance with the results of Hadinoto et al. (2006), which were obtained without the inclusion of the phospholipids in the formulation. Hence, the presence of the phospholipids does not alter how increasing the nanoparticles concentration influences the degree of hollowness of the large hollow nanoparticles aggregates. However,

Table 2

A summary of the experimental results of Hadinoto et al. (2006)

Nanoparticles	Nanoparticles concentration (% , w/w)	$\rho_e/\rho_{\text{true}}^a$ ($\pm 13\%$, $\pm 10\%$)	$\rho_e/\rho_{\text{true}}^b$ ($\pm 10\%$)	d_g (μm) ($\pm 10\%$)	d_a (μm) ($\pm 5\%$)
Polyacrylate $140 \pm 10 \text{ nm}$	0.80	0.15	0.05	11.6	2.8
	0.92	0.16	0.07	10.6	3.1
	1.20	0.15	0.05	9.5	2.5
	1.50	0.15	0.17	6.7	3.1
	2.40	0.16	0.17	7.9	3.7
	3.20	0.15	0.08	8.3	2.6
Silica $20 \pm 10 \text{ nm}$	0.23	0.08	0.04	9.0	2.7
	0.35	0.08	0.05	7.9	2.6
	0.47	0.15	0.08	7.9	3.4
	0.82	0.22	0.10	5.4	2.6
	1.41	0.23	0.16	4.3	2.6
	1.88	0.29	0.10	5.1	2.4

^a From tap density measurement, ψ^{tap} .

^b From the ratio of $(d_a/d_g)^2$, ψ^{dia} .

contrary to the results of Tsapis et al. (2002) and Hadinoto et al. (2006), our results indicate that the magnitude of the degree of hollowness (ψ^{dia}) and the particle size are no longer independent of the size of the nanoparticles in the presence of the phospholipids (Table 1). At the same nanoparticles concentration, the geometric diameter of the particles obtained from the spray drying of the 70 ± 40 nm nanoparticles is significantly larger than that of the 170 ± 80 nm nanoparticles, whereas their aerodynamic diameters remain the same. Accordingly, the degree of hollowness (ψ^{dia}), which is determined from the magnitude of $(d_a/d_g)^2$, varies for the two nanoparticles. The competitive adsorption between the nanoparticles and the phospholipids, which is expected to vary for different size nanoparticles, is postulated to influence the shell formation process, resulting in the variation in the size of the spray-dried particles.

The respirable fine particle fraction ($d_a \leq 4.7 \mu\text{m}$) of the spray-dried particles (determined using the cascade impactor at 28.3 L/min) is approximately $20 \pm 10\%$, and remains constant for a wide range of nanoparticles concentrations. The constant respirable fine particle fraction is consistent with the constant aerodynamic diameter as a function of the nanoparticles concentration (Table 1). The magnitude of the respirable fine particle fraction of the spray-dried particles is comparable to the values reported in Tsapis et al. (2002) and Sham et al. (2004) at 60 L/min, in which a similar type of particles was formulated. A flow rate of 60–90 L/min in the cascade impactor represents a more realistic value for the human inhalation flow rate in a dry powder inhaler (Sham et al., 2004). The higher inhalation flow rate has been shown to lead to an enhanced dispersion of the particle aggregates off the dry powder inhaler (French et al., 1996; Li et al., 1996). Therefore, an increase in the magnitude of the respirable fine particle fraction of the spray-dried particles is expected at a higher inhalation flow rate.

3.3. Effects of increasing phospholipids concentration

To further investigate the effects of incorporating the phospholipids in the formulation of the large hollow nanoparticulate aggregates, a study on the effects of increasing the phospholipids concentration on the morphology and degree of hollowness of the spray-dried particles is conducted. A constant amount of the nanoparticles is spray dried in the presence of a wide range of phospholipids concentrations (i.e. up to 58% of the total solid content). The nanoparticles concentration is maintained at the concentration threshold necessary to facilitate the formation of the large hollow nanoparticulate aggregates (1.6 g/200 mL). Nanoparticles of different sizes and chemical nature are used in the experiment (i.e. the 50 ± 30 and 160 ± 40 nm polyacrylate nanoparticles, and the 50 ± 30 nm silica nanoparticles). A summary of the experimental results for the degree of hollowness and particle size distribution is provided in Table 3.

The 160 ± 40 nm polyacrylate nanoparticles, which are synthesized using only MMA as the monomer, are different in their chemical nature compared to the 50 ± 30 nm nanoparticles, which are synthesized by the tetrapolymerization of the MMA, Ba, AA, and MeOPEGMA monomers. As a result, the 160 ± 40 nm nanoparticles exhibit a different polymer backbone structure relative to the 50 ± 30 nm nanoparticles. In addition, they also lack the steric stability provided by the MeOPEGMA chains. Due to the dissimilarity in the chemical nature of the three nanoparticles, the degree of hollowness (ψ^{tap} , ψ^{dia}) and the geometric size of the spray-dried particles, at zero phospholipids concentration, vary for each nanoparticles type (Table 3). In the absence of the phospholipids, the variations in the degree of hollowness and size, among the three nanoparticles, signify the role of the chemical nature of the nanoparticles in the large hollow nanoparticulate aggregates formation.

Table 3

A summary of the experimental results for the effects of the phospholipids concentration in the presence of the nanoparticles

Nanoparticles	Solid concentration (%, w/w)	Phospholipids (% of total solid)	$\rho_e/\rho_{\text{true}}^a$ ($\pm 13\%$)	$\rho_e/\rho_{\text{true}}^b$ ($\pm 10\%$)	Mean d_g (μm) ($\pm 10\%$)	Median d_g (μm)	Mode d_g (μm)	d_a (μm) ($\pm 5\%$)
Polyacrylate 50 ± 30 nm	0.80	0	0.19	0.04	11.9	7.9	8.9	2.6
	0.87	6	0.19	0.04	11.2	7.5	8.9	2.4
	0.92	11	0.19	0.07	8.8	6.0	7.1	2.7
	1.02	20	0.18	0.06	9.8	7.0	8.0	2.7
	1.12	27	0.20	0.05	11.4	8.5	10.0	2.9
	1.33	38	0.16	0.04	12.9	8.2	10.0	2.7
Polyacrylate 160 ± 40 nm	0.80	0	0.43	0.13	8.6	7.0	5.7	3.5
	1.02	20	0.36	0.07	9.8	7.5	7.1	2.9
	1.23	33	0.19	0.05	9.6	7.1	7.1	2.4
	1.63	50	0.14	0.04	9.5	7.1	7.1	2.1
	1.94	58	0.16	0.03	12.9	8.7	7.1	2.7
Silica 20 ± 10 nm	0.40	0	0.15	0.08	7.9	3.0	3.0	3.4
	0.46	11	0.20	0.09	6.8	4.0	4.5	3.0
	0.51	20	0.25	0.12	8.1	5.1	6.3	4.2
	0.61	33	0.30	0.16	6.5	4.0	4.5	3.9

^a From tap density measurement, ψ^{tap} .

^b From the ratio of $(d_a/d_g)^2$, ψ^{dia} .

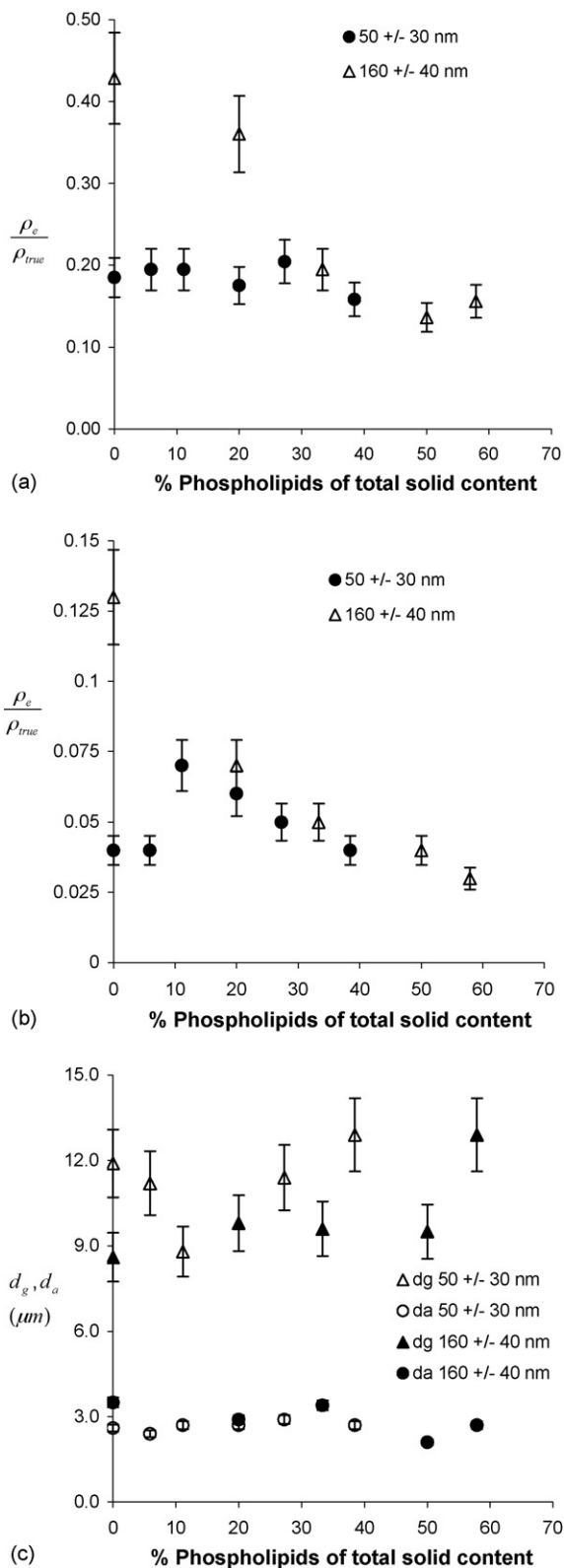


Fig. 6. Spray-dried particles of the 50 ± 30 and 160 ± 40 nm polyacrylate nanoparticles: (a) the degree of hollowness determined from the tap density, ψ^{tap} , (b) the degree of hollowness determined from the diameters, ψ^{dia} and (c) geometric and aerodynamic diameters.

For the 50 ± 30 nm nanoparticles, Fig. 6a shows that the degree of hollowness (ψ^{tap}) of the spray-dried particles is not affected by the increase in the phospholipids concentration. Recognizing the limitation of the tap density measurement, the trend in the degree of hollowness is re-evaluated using the value of ψ^{dia} . Despite the discrepancy in the magnitudes of ψ^{tap} and ψ^{dia} , Fig. 6b shows that the trend is consistent with the results presented in Fig. 6a, as the variation in the degree of hollowness (ψ^{dia}) of the spray-dried particles is still within its experimental uncertainties. For the 160 ± 40 nm nanoparticles, on the other hand, the degree of hollowness (ψ^{tap} , ψ^{dia}) is shown to increase with increasing phospholipids concentration in both Fig. 6a and b. The results indicate that the trend in the degree of hollowness, as a function of the phospholipids concentration, depends on the size and chemical nature of the nanoparticles. The significance of the size and chemical nature influence on the effects of increasing the phospholipids concentration is reinforced by the results of the spray-dried 20 ± 10 nm silica nanoparticles. In contrast to the polyacrylate nanoparticles, the degree of hollowness (ψ^{tap} , ψ^{dia}) of the spray-dried silica particles is shown to decrease with increasing phospholipids concentration (Table 3).

More importantly, Fig. 6c indicates that both the geometric and aerodynamic diameters of the spray-dried particles are not significantly affected by the change in the phospholipids concentration. The respirable fine particle fraction of the spray-dried particle also remains at approximately $20 \pm 10\%$ for a wide range of phospholipids concentrations. In addition, the particle size distribution (Table 3) indicates that increasing the phospholipids concentration does not lead to an increased production of the fine particles. Therefore, the degree of hollowness of the large hollow nanoparticulate aggregates is best controlled by varying the phospholipids concentration, instead of varying the nanoparticles concentration, because it does not jeopardize the particle size distribution of the spray-dried particles.

4. Conclusions

The results of our study demonstrate that the inclusion of the phospholipids in the formulation of the large hollow nanoparticulate aggregates leads to an accumulation of the phospholipids at the surface of the spray-dried particles. The presence of the phospholipids does not alter the morphology or the physical state of the spray-dried particles. Furthermore, the trend in the degree of hollowness of the large hollow nanoparticulate aggregates, as a function of the nanoparticles concentration, is not affected by the presence of the phospholipids. However, the inclusion of the phospholipids results in the size and the degree of hollowness of the spray-dried particles being dependent on the nanoparticles size. The results also indicate that increasing the nanoparticles concentration high above the threshold value leads to an increased production of the fine particles, which exhibit a higher effective particle density, and this leads to a diminished production of the large hollow nanoparticulate aggregates. On the other hand, our study on the effects of the phospholipids concentration shows that the degree of hollowness can be controlled

by varying the phospholipids concentration, without affecting the particle size distribution and the respirable fine particle fraction of the spray-dried particles. Therefore, it is more favorable to control the degree of hollowness of the large hollow nanoparticulate aggregates by varying the phospholipids concentration. The trend in the degree of hollowness, as a function of the phospholipids concentration, is found to depend on the chemical nature and size of the nanoparticles. Lastly, the sole reliance on the tap density measurement is not adequate to accurately capture the variation in the degree of hollowness of the spray-dried particles.

Acknowledgements

The authors would like to thank Koh Guoxiong and Chong Wei Ming for their contribution in the spray drying experiments and particle characterizations, and A*STAR (Agency for Science, Technology and Research) of Singapore, Grant ICES/05-122001, for funding this work.

Appendix A. Test of statistical significance

See Table A.1.

A.1. Methods

1. For the test of statistical significance, n number independent experimental measurements of samples 1 and 2 are purposely conducted to form n number independent replicates. The parameters of interest are the mean values of d_g , d_a , because the degree of hollowness is proportional to the ratio of $(d_a/d_g)^2$.
2. For the effects of the nanoparticles concentration, the test of statistical significance is conducted using the 70 ± 40 nm polyacrylate as the representative sample. The t -test analysis is conducted at the highest (subscript 2) and lowest (subscript 1) nanoparticles concentrations (Table A.1). For the

effects of the phospholipids concentration, the t -test analysis is conducted using the 160 ± 40 nm polyacrylate nanoparticles and the 20 ± 10 nm silica nanoparticles as the representative samples. Similarly, the test is conducted at the highest (subscript 2) and lowest (subscript 1) phospholipids concentrations. The statistical significance of the effects of increasing the nanoparticles and phospholipids concentrations on the degree of hollowness can therefore be determined from the t -test results.

3. The hypothesis to be tested is $H_1: \mu_1 - \mu_2 = 0$, which implies that the population means of samples 1 and 2 are equal, such that the difference in the sample means x_1 and x_2 is statistically insignificant.
4. For $\alpha = 0.05$, we would reject the hypothesis H_1 when $t_{\text{calc}} < t_{\alpha/2, \text{D.O.F.}}$ or when $t_{\text{calc}} < -t_{\alpha/2, \text{D.O.F.}}$.
5. If the hypothesis H_1 can be rejected, then there is a strong statistical evidence that the difference in the sample means of d_g , d_a (obtained from samples 1 and 2) are statistically significant, and not due to a random occurrence.

A.2. Results

The t -test results at the α value of 0.05 (Table A.1) indicate that the t_{calc} values for the d_g data are always larger than the values of $\pm t_{\alpha/2, \text{D.O.F.}}$, which signify the statistical significance of the reported trend in the geometric diameter. In addition, the t -test results of the d_a data (where $-t_{\alpha/2, \text{D.O.F.}} < t_{\text{calc}} < t_{\alpha/2, \text{D.O.F.}}$, hence they are statistically insignificant) reiterate the conclusion that the aerodynamic diameter is hardly influenced by the change in the nanoparticles or phospholipids concentrations. In conclusion, the t -test results of the geometric diameter have shown that the reported trends in the degree of hollowness (which is proportional to the square ratio of the aerodynamic to geometric diameters) as a function of the nanoparticles and phospholipids concentrations are statistically significant and not due to a random occurrence.

Table A.1

	x_1	s_1	x_2	s_2	$n_1 = n_2$	D.O.F.	$\alpha = 0.05$ $t_{\alpha/2, \text{D.O.F.}}$	t_{calc}
Polyacrylate								
d_g 70 ± 40 nm	13.7	1.1	7.9	1.0	6	12	2.179	9.557
d_a 70 ± 40 nm	3.4	0.6	3.2	0.5	6	12	2.179	0.627
d_g 160 ± 40 nm	8.6	1.3	12.4	1.6	8	15	2.131	-5.214
d_a 160 ± 40 nm	3.3	0.6	3.0	0.6	8	16	2.120	1.000
Silica								
d_g 20 ± 10 nm	0	0.9	6.5	0.9	8	16	2.120	2.444
d_a 20 ± 10 nm	3.2	0.4	3.6	0.5	8	16	2.120	-1.767

Nomenclature: $x_{1,2}$ = the mean of samples 1, 2; $\mu_{1,2}$ = the mean of populations 1, 2; $s_{1,2}$ = the standard deviation of samples 1, 2; $n_{1,2}$ = the number of independent replicates of samples 1, 2; D.O.F. = the degree of freedom; α = the probability of error, alpha parameter, in the t -test.

$$t_{\text{calc}} = \frac{x_1 - x_2}{\sqrt{(s_1^2/n_1) + (s_2^2/n_2)}} \quad (\text{A.1})$$

$$\text{D.O.F.} = \frac{((s_1^2/n_1) + (s_2^2/n_2))^2}{(s_1^2/n_1)^2/(n_1 + 1) + (s_2^2/n_2)^2/(n_2 + 1)} - 2 \quad (\text{A.2})$$

Montgomery and Runger (1999).

References

- Adler, M., Unger, M., Lee, G., 2000. Surface composition of spray-dried particles of bovine serum albumin/trehalose/surfactant. *Pharm. Res.* 17, 863–870.
- Ahsan, F., Rivas, I.P., Khan, M.A., Suarez-Torres, A.I., 2002. Targeting to macrophages: role of physicochemical properties of particulate carriers-liposomes and microspheres on the phagocytosis by macrophages. *J. Controlled Release* 79, 29–40.
- Bosquillon, C., Lombry, C., Preat, V., Vanbever, R., 2001. Influence of formulation excipients and physical characteristics of inhalation dry powders on their aerosolization performance. *J. Controlled Release* 70, 329–339.
- Cook, R.O., Pannu, R.K., Kellaway, I.W., 2005. Novel sustained release microspheres for pulmonary drug delivery. *J. Controlled Release* 104, 79–90.
- Dellamary, L.A., Tarara, T.E., Smith, D.J., Woelk, C.H., Adractus, A., Costello, M.L., Gill, H., Weers, J.G., 2000. Hollow porous particles in metered dose inhalers. *Pharm. Res.* 17, 168–174.
- Edwards, D.A., Hanes, J., Caponetti, G., Hrkach, J., Ben-Jebria, A., Eskew, M., Mintzes, J., Deaver, D., Lotan, N., Langer, R., 1997. Large porous particles for pulmonary drug delivery. *Science* 276, 1868–1871.
- Eerikainen, H., Watanabe, W., Kauppinen, E.I., Ahonen, P.P., 2003. Aerosol flow reactor method for synthesis of drug nanoparticles. *Eur. J. Pharm. Biopharm.* 55, 357–360.
- Evora, C., Soriano, I., Rogers, R.A., Shakesheff, K.M., Hanes, J., Langer, R., 1998. Relating the phagocytosis of microparticles by alveolar macrophages to surface chemistry: the effect of 1,2-dipalmitoylphosphatidylcholine. *J. Controlled Release* 1, 143–152.
- French, D.L., Edwards, D.A., Niven, R.W., 1996. The influence of formulation on emission, deaggregation, and deposition of dry powders for inhalation. *J. Aerosol Sci.* 27, 769–783.
- Govender, T., Stolnik, S., Garnett, M.C., Illum, L., Davis, S.S., 1999. PLGA nanoparticles prepared by nanoprecipitation: drug loading and release studies of a water soluble drug. *J. Controlled Release* 57, 171–185.
- Grenha, A., Seijo, B., Lopez, C.R., 2005. Microencapsulated chitosan nanoparticles for lung protein delivery. *Eur. J. Pharm. Sci.* 25, 427–437.
- Hadinoto, K., Phanapavudhikul, P., Zhu, K., Tan, R.B.H., 2006. Novel formulation of large hollow nanoparticles aggregates as potential carriers in inhaled delivery of nanoparticulate drugs. *Ind. Eng. Chem. Res.* 45, 3697–3706.
- Hinds, W.C., 1982. *Aerosol Technology*. Wiley, New York.
- Hyvönen, S., Peltonen, L., Karjalainen, M., Hirvonen, J., 2005. Effect of nanoprecipitation on the physicochemical properties of low molecular weight poly(L-lactic acid) nanoparticles loaded with salbutamol sulphate and beclomethasone dipropionate. *Int. J. Pharm.* 295, 269–281.
- Jones, B.G., Dickinson, P.A., Gumbleton, M., Kellaway, I.W., 2002. Lung surfactant phospholipids inhibit the uptake of respirable microspheres by the alveolar macrophage NR8383. *J. Pharm. Pharmacol.* 54, 1065–1072.
- Kipp, J.E., 2004. The role of solid nanoparticle technology in the parenteral delivery of poorly water-soluble drugs. *Int. J. Pharm.* 284, 109–122.
- Lalka, D., Griffith, R.K., Cronenberger, C.L., 1993. The hepatic first-pass metabolism of problematic drugs. *J. Clin. Pharmacol.* 33, 657–659.
- Lee, J.H., 2003. Drug nano and microparticles processed into solid dosage forms: physical properties. *J. Pharm. Sci.* 92, 2057–2068.
- Li, W.I., Perzl, M., Heyder, J., Langer, R., Brain, J.D., Englemeier, K.H., Niven, R.W., Edwards, D.A., 1996. Aerodynamics and aerosol particle deaggregation phenomena in model oral-pharyngeal cavities. *J. Aerosol Sci.* 27, 1269–1286.
- Liang, H., Shinohara, K., Minoshima, H., Matsushima, K., 2001. Analysis of constant rate period of spray drying slurry. *Chem. Eng. Sci.* 56, 2205–2213.
- Lukasiewicz, S.J., 1989. Spray-drying of ceramic powders. *J. Am. Ceram. Soc.* 72, 617–624.
- Maa, Y.F., Nguyen, P.A.T., Hsu, S.W., 1998. Spray drying of air-liquid interface sensitive recombinant human growth hormone. *J. Pharm. Sci.* 87.
- Makino, K., Yamamoto, N., Higuchi, K., Harada, N., Ohshima, H., Terada, H., 2003. Phagocytic uptake of polystyrene microspheres by alveolar macrophages: effects of the size and surface properties of the microspheres. *Colloid Surf. B* 27, 33–39.
- Montgomery, D.C., Runger, G.C., 1999. *Applied Statistics and Probability for Engineers*. John Wiley and Sons, New York, pp. 388–394.
- Moon, W.S., Chung, H.J., Park, S.B., Woo, S.I., 2000. Effects of lead acetate concentration on the droplet size in liquid source misted chemical decomposition. *Thin Solid Films* 358, 86–89.
- Pang, Y.N., Sakagami, M., Byron, P.R., 2005. The pharmacokinetics of pulmonary insulin in the in-vitro isolated perfused rat lung: implications of metabolism and regional deposition. *Eur. J. Pharm. Sci.* 25, 369–378.
- Patel, A.A., White, C.M., Coleman, C.I., 2005. Exubera—an orally inhaled insulin. *Formulary* 40, 429.
- Phanapavudhikul, P., Waters, J.A., Ortiz, E.S., 2002. Para-magnetic composite microparticles as heavy metal ion-exchangers. *Eur. Cells Mater.* 3, 118–121.
- Raula, J., Eerikainen, H., Kauppinen, E.I., 2004. Influence of the solvent composition on the aerosol synthesis of pharmaceutical polymer nanoparticles. *Int. J. Pharm.* 284, 13–21.
- Sacchetti, M., Van Oort, M.M., 1996. In: Hickey, A.J. (Ed.), *Spray Drying and Supercritical Fluid Particle Generation Techniques. Inhalation Aerosols—Physical and Biological Basis for Therapy*. Marcel Dekker, New York, pp. 337–384.
- Scherer, G.W., 1990. Theory of drying. *J. Am. Ceram. Soc.* 73, 3–14.
- Sham, J., Zhang, Y., Finlay, W.H., Roa, W.H., Lobenberg, R., 2004. Formulation and characterization of spray-dried powders containing nanoparticles for aerosol delivery to the lung. *Int. J. Pharm.* 269, 457–467.
- Shargel, L., Yu, A.B., 1999. *Applied Biopharmaceutics & Pharmacokinetics*, fourth ed. McGraw Hill, New York.
- Steckel, H., Brandes, H.G., 2004. A novel spray drying technique to produce low density particles for pulmonary delivery. *Int. J. Pharm.* 278, 187–195.
- Teixeira, M., Alonso, M.J., Pinto, M.M.M., Barbosa, C.M., 2005. Development and characterization of PLGA nanospheres and nanocapsules containing xanthone and 3-methoxyxanthone. *Eur. J. Pharm. Biopharm.* 59, 491–500.
- Tsapis, N., Bennet, D., Jackson, B., Weitz, D.A., Edwards, D.A., 2002. Trojan particles: large porous carriers of nanoparticles for drug delivery. *Proc. Natl. Acad. Sci. U.S.A.* 99, 12001–12005.
- Vanbever, R., Mintzes, J., Wang, J., Nice, J., Chen, D., Batycky, R., Langer, R., Edwards, D.A., 1999. Formulation and physical characterization of large porous particles for inhalation. *Pharm. Res.* 16, 1735–1742.